Design and Building of a Multi-finger Robotic Hand Prototype for Grip Control

Sergio A. Pertuz [1,*], Cesar A. Peña [2], and Cristhian I. Riaño [2]

[1] Computer Science Faculty, Technical University of Dresden, Dresden, Germany
[2] Department of Mechatronic, Industrial and Mechanical Engineering, University of Pamplona, Pamplona, Colombia;
Email: {cesarapc, cristhian.riano}@unipamplona.edu.co (C.A.P., C.I.R.)
*Correspondence: sergio.pertuz@tu-dresden.de (S.A.P.)

***Abstract*—This paper presents the design and construction of a multi-finger biometric robotic hand prototype that can be used as an end effector in processes that require dexterous grasping of objects. The research aims to obtain an optimized mechanism that manages to emulate the movements of a hand using a reduced number of joints and links. A rigid mechanism with actuators in the palm is mathematically modeled and kinematically verified through a functional grip application. A biologically inspired optimization algorithm is employed in the dimensional optimization of the mechanism to follow a trajectory profile that defines the type of grip. As a result, a robotic hand is obtained with a proportion that does not exceed 10% of the dimensions of a human hand, which integrates a mechanism with 7 Degrees of freedom (DOF) and 16 joints and a trajectory control that guarantees different types of grip. Different grips presented in this document show the dexterity of the hand, given by the kind of rigid mechanism and trajectory profile tracking. The adduction and abduction movements of the hand extend their usefulness to reproduce different types of grips.**

***Keywords*—robotics, hand, multi-fingered, mechatronic hand, genetic algorithms**

I. Introduction

Different studies are focused on the design and construction of robotic hands, resulting in significant contributions in emulating human behavior to manipulate objects [1, 2]. The human hand has a high anthropometric complexity and 20-DoF [3]. Reaching the same level of human dexterity with robotic systems is a challenge that requires integrating mechanisms, actuators, and control systems in a reduced space [4]. One characteristic to measure the performance of designs in robotic hands is proposing a metric on the type of grip it exercises; therefore, the large number of works on robotic hands have substantial differences, and there are still opportunities for study [5].

This research proposes creating a functional mechanism with reduced degrees of freedom with integrated grip control. The contributions of this research consist in reducing the level of complexity both in manufacturing and in the technical elements involved in the prototype of the robotic hand, a hand is projected with the possibility of being coupled with other open kinematics robotic systems such as anthropomorphic robots to handle different types of objects and perform complex tasks that require dexterity, precision, and adaptability in grips, functions that are difficult to achieve with conventional end effectors.

The human hand can perform numerous types of grips [6], but in the design of a robotic hand prototype, it is necessary to limit the types of grip to its functional objective, these are issues that depend on the tasks to be developed [7]. However, studies in this regard suggest that precision grips are favorable for interaction tasks [8]. One strategy in constructing the conceptual model consists of establishing metrics on the grasping mechanism that allow the creation of a selection criterion, either based on the points of contact with the object or on the geometric relations of grasping [9]. The required functionality is not associated with a specific object type but is close to a generalized grip to a particular curve profile.

Within this line of research, two large groups of mechanisms called rigid and soft stand out for constructing multi-fingered robotic hands [10]. Mechanisms with a soft grip type can help handle delicate objects [11]. However, adaptability to different kinds of grip can be challenging [12]. Its operating principle is mainly based on flexible pneumatic actuators, using materials such as rubber or polymers [13]. The grip force in this type of mechanism can be derived from controlling the magnitude of the curvature, but the gripping efficiency can be compromised [14]. On the other hand, in rigid mechanisms, we find variants that simplify the mechanism and be multipurpose in object manipulation activities. For example, when the gripping conformability of an object is out of the control strategy [15], the advantages can be obtained by designing the surfaces that make up the device that conforms to the surface [16], however, the degrees of freedom along with the number of reduced joints influence their dexterity.

Trying to replicate the DOF of human hands in robotic systems is a complex task [17], in many cases, it is necessary to implement an actuator for each projected degree of freedom with the mitigation of being able to use reduced space for its installation [18]. There are several design approaches, such as the inclusion of actuators in the

Manuscript received February 8, 2023; revised March 22, 2023; accepted May 25, 2023.

forearms and transmitting movements through tendons [19], motors directly coupled to the joints, rod mechanisms that transmit movement through a curved profile [20]. In finger mechanisms based on bars as actuating elements, the degrees of freedom achieved in multi-fingered hands bring the possibilities of controlling the type of grip closer through a defined trajectory.

From the design perspective, these devices present substantial limitations in their implementation as emulators because of the limited space available for each articulation. Movement transmission devices are needed to avoid interference with this space limitation [21]. The proposed robotic hand uses four connected stick mechanisms to imitate fingers' flexion and extension movements [22]. In his study, Cobos [23] presents sub-perform movements of flexion and inflection, establishing a relationship between each phalanx angle to achieve natural grip and gesture movements. Given the nature of this mechanism, the phalanx dimensions are only known in this case. Other designs are initially unknown (8 unknown dimensions). The number of unknown dimensions is higher than the number of available equations, which is why a heuristic optimization method has been proposed [24].

A design perspective found in recent research is to design the robotic hand as simplified as possible and to allow many grips to be obtained [25]. Some approaches that reduce the complexity of the designs maintain versatility in some types of grips; however, it is noteworthy that the control strategies can also become simplified in practice due to the reduction in the number of actuators and the number of embedded sensors on devices [26].

Based on these contributions and previous work, it is determined that for the project, the best option is to propose a rigid multi-finger mechanism and implement a control that allows obtaining different types of grip [27]. The dimensions and geometry of the prototype are defined both by the shape of the actuators and by the tray sector profile designed with a functional purpose. These characteristics can be perfectly optimized [28] by using Genetic Algorithms (GA) for this task as heuristic and adaptive search techniques based on genetic conjectures and natural selection, which emulate evolutionary processes to solve this type of problem [29].

This research aimed to obtain a mechanism with fewer degrees of freedom that maintain grip performance similar to that of a human hand. Below is the development of a simplified mechanism based on seven degrees of freedom that can be used as a final effector in tasks that require dexterity. The profile of the projected trajectory for the finger mechanism is compared with the actual trajectory, yielding a performance criterion. The method used to achieve the ManUPA multi-finger robotic hand is presented below.

II. Related Works

When a search is carried out on robotic hands, research works in recent years are found due to the interest in robotizing human behavior. An end effector is projected with high levels of dexterity for the manipulation of different objects, and that has a feedback grip control; In this sense, the search for related jobs can be delimited to certain degrees of anthropomorphism associated with DOF to define the levels of dexterity and functional characteristics of a multi-fingered hand. Next, investigative works of 5-fingered hands are presented, which present some synthesis, either in degrees of freedom actuators or grip control that, due to their results and contribution, are references for this and future works.

The Belgrade/USC hand, considered one of the first hands with five fingers, has pressure sensors in each of its fingers. A single actuator controlled the grip, causing the pressure on all fingers to be distributed evenly across all your fingers when grasping an object. The improved version has 4-DOF with 18 joints [30]. TUAT/Karlsruhe humanoid hand, designed for a humanoid robot, has five fingers out of 4 that are the same and 20-DOF controlled by a single actuator [31]. These two hands are benchmarks for grip control based on a single actuator.

Robonaut Robotic hand has five fingers, and 12-DOF plus 2-DOF on the wrist gives 14-DOF. The hand robotic, made for spatial work, have motors located externally and transmit the movement through a flexible transmission, finally, the rotational movement becomes linear movement by spindles in hand [32].

The ultralight anthropomorphic hand has five fingers and 10-DOF on the arrow and 3-DOF on the wrist, pneumatically controlled, it has integrated actuators in the fingers that reach 12 N of pressure at the fingertips. It is lightweight and adaptable to different processes [33].

Gifu Robotic Hand has 3 degrees of freedom in four fingers and 4-DOF in the thumb, each finger has three joints. The hand has a tactile sensor and six-axis force sensors [34].

DLR-HIT-Hand II is a hand with five identical fingers with fifteen degrees of freedom. Each finger has 3-DOF and four joints, the last two joints are mechanically coupled. All actuators are fully integrated into the finger's base [35]. KITECH-Hand is one of the most affordable commercial hands. It has four fully actuated 16-DOf fingers [36].

ILDA hand is a robotic hand with integrated drives with 15-DOF, 20 joints, and a fingertip force of 34 N. Its main characteristic is the force vs. weight relationship and dexterity in tool handling tasks [37].

The research presented in this document shows the development of a five-fingered hand simplified to 7-DOF and 16 joints that manages to reproduce grips with skill. The design has positive effects by reducing the number of actuators to perform the movements, integrating the actuators inside the hand, and having grip control through a trajectory executed on each finger utilizing a four-bar mechanism. Reducing the number of actuators and controlling a more significant number of degrees of freedom minimize energy consumption and weight in hand and make numerous applications viable.

III. The Material and Method

A. Applied Mechanism Design and Robotic Fingers

In the design of a rigid multi-finger mechanism, a decision must be made between the different forms of actuation and transmission mechanisms to move the robotic joints. Two possibilities are contemplated when choosing the venues:

- Engines might be placed near the articulations, sometimes, they can be integrated into the fingers [36].
- Placing the engines or performers in the palm, forearm, or any external position to the fingers by using movement transmissions [38].

For the first possibility, when placing the actuators near the joint of each finger, it gets more challenging to accomplish the objective of preserving the actual dimensions of a human hand, thus, in this prototype, a second option was chosen, which is named "Remote performance", this one requires mechanic transmissions that can be broken down into two kinds:

- Flexible transmission: where joints are distorted and adaptable by using tendons or cables to transmit movement. It has a limitation, it cannot perform high precision grip of small objects with the fingertips, this is produced because some kinds of cable stretch out or some move inside the ducts, causing some placement errors [39]. Finally, there is a problem with controlling the fingertips' placement because of the lack of systematic linearity.
- Rigid Transmission: Generally, it refers to transmission movement mechanisms of sticks and gears. Among its advantages is its rigidness, which makes it long-lasting and allows estimating a precise fingertip placement [40]. It has some limitations, when it detects any interference among its components, its mechanism gets tangled up.

Finally, it was decided to implement a mechanism for the fingers with Rigid Transmission; for this mechanism, a trajectory profile will be created that determines the specific type of grip. The Finger Mechanism used in each degree of freedom of the ManUPA is detailed below.

1) Fingers mechanism

The mechanic system involves two mechanisms, each one with four connected links; three of the links that make up this mechanic system are the three phalanges of each finger, without the thumb, because this one is only employed for a four-links mechanism. Each phalange is integrated with the others, respecting the restrictions shown in Table I.

The developed mechanism is illustrated in Fig. 1, links one, three, and five, illustrated in Fig. 1(b) correspond to the distal, medium, and proximal phalanxes. Links two and four transmit movement from one phalanx to the next. The first movement is angular, performed in a concentric revolution joint to the arch illustrated in the connection mechanism in Fig. 1(a). Each finger needs one actuator to be activated. In this case, an endless winder transmission is included, giving the finger an auto-inhibition feature.

TABLE I. Fingers' Mechanism Angular Restrictions of Interphalangeal Joints.

Joint	Flexion / Extension Restriction
Metacarpal-phalange (θ_1)	0–90 °
Proximal inter-phalangeal (θ_2)	0–100 °
Distal inter-phalange (θ_3)	0–90 °

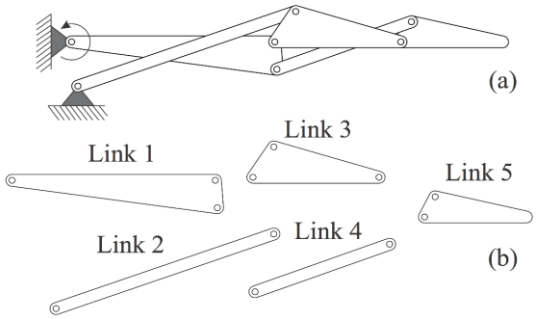

Figure 1. Fingers' mechanic system diagram. (a) Assembled. (b). Exploited

One of the limitations of this design is that the aim is to preserve human hand dimensions. For doing this, information about phalanx dimensions has been gathered, in general terms, this information was provided by the study of O. Binvignat *et al.* [41].

This mechanism moves to undertake the proper trajectory to perform different kinds of grip, the fingertips' trajectory is illustrated as a dotted line in Fig. 2.

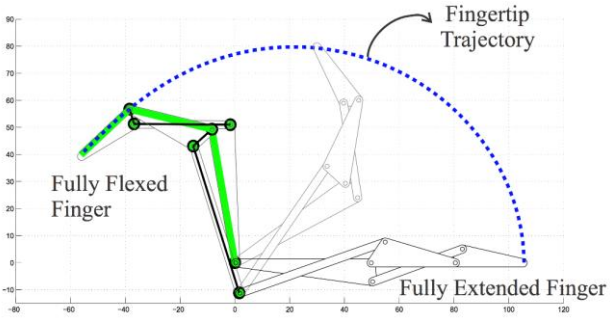

Figure 2. The fingertip trajectory

In the study of Cobos [23], the author proposes that when there is the aim of sub-performing other joints with flexion and extension finger movements, it is necessary to organize the angles of each phalanx $\theta 2$ and θ_3 so that they can have a movement connection concerning the entrance θ_1 (see Table I). These relations are indicated in Eqs. (1) and (2).

$$\theta_1 = \frac{4}{3}\theta_2 \quad (1)$$

$$\theta_2 = \frac{3}{2}\theta_3 \quad (2)$$

The angles θ_1 and θ_2 are illustrated in Fig. 3(a). In Fig. 2, their relations θ_1, θ_2, and θ_3 do not accomplish the connections proposed by Cobos [42].

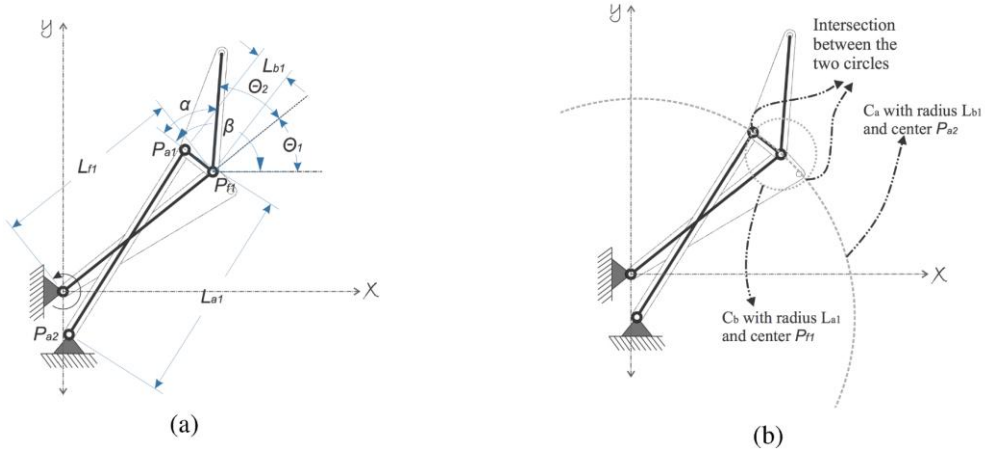

Figure 3. Fingers' mechanic system. (a) Finger's 4-stick mechanism graphic kinematic representation (b) Graphic representation of Ca and Cb.

A kinematic analysis is required to complement the design of the mechanism, it is necessary to verify through this analysis the dimensions of the links that maintain the connections. The kinematic analysis performed is presented below.

2) Mechanism's kinematic analysis

The kinematic analysis of the mechanism is performed by disconnecting the two 4–stick mechanisms and studying them individually. Considering the two of them are the same, this analysis is enough to understand all the mechanic systems of the finger. Links 1–3 represents the first 4-stick mechanism, broken down in its dimension in Fig. 3.

Fig. 3(a), illustrates the parameters that shape the mechanism, and this one is located in a random position to be studied. Now parameters are: L_{f1}, L_{a1}, L_{b1}, the point P_{a2}, and $\theta 1$. It is necessary to know the mechanism's output (θ_2) for design purposes. The point P_{f1} is estimated through vector analysis, as shown in Eq. (3).

$$P_{f1} = L_{f1}\langle \cos\theta_1\, \hat{\imath} + \cos\theta_1 \hat{\jmath}\rangle \tag{3}$$

It is necessary to locate point P_{a2}, which could be interpreted as the intersection among the two radius circles L_{a1} and L_{b1}, with the center in P_{a2} and P_{f1}, respectively. They will be named C_a y C_b. Fig. 3(b) illustrates the represented circles graphically with the Eqs. (4) and (5)

$$C_a: x^2 + y^2 + D_a x + E_a y + F_a = 0 \tag{4}$$

$$C_b: x^2 + y^2 + D_b x + E_b y + F_b = 0 \tag{5}$$

where:

$$D_a = -2P_{a2}\hat{\imath} \tag{6}$$

$$E_a = -2P_{a2}\hat{\jmath} \tag{7}$$

$$F_a = (P_{a2}\hat{\imath})^2 + (P_{a2}\hat{\jmath})^2 - {L_{a1}}^2 \tag{8}$$

$$D_b = -2P_{f1}\hat{\imath} \tag{9}$$

$$E_b = -2P_{f1}\hat{\jmath} \tag{10}$$

$$F_b = (P_{f1}\hat{\imath})^2 + (P_{f1}\hat{\jmath})^2 - {L_{b1}}^2 \tag{11}$$

The following step is to find the intersections between both circles and select the option that solves the mechanism. Reducing the Eqs. (4) and (5), the result is:

$$(D_a - D_b)\, x + (E_a - E_b)\, y + F_a - Fb = 0 \tag{12}$$

Then clearing the formula, from Eq. (12) it is obtained:

$$y = \frac{(D_b - D_a)x + F_b - F_a}{E_a - E_b} \tag{13}$$

And replacing Eq. (13) in Eq. (4)

$$\left(\frac{(D_a - D_b)^2}{(E_a - E_b)^2} + 1\right)x^2 + \left(D_a - \frac{E_a(D_a - D_b)}{E_a - E_b} + \frac{2(D_a - D_b)(F_a - F_b)}{(E_a - E_b)^2}\right)x$$

$$+F_a + \frac{(F_a - F_b)^2}{(E_a - E_b)^2} - \frac{E_a(F_a - F_b)}{(E_a - E_b)} = 0 \tag{14}$$

It is possible to appreciate a quadratic equation in Eq. (14), which has found that two solutions of minimums value are chosen, this happens because the finger moves only in the first two quadrants of the coordinated axes. This solution is valid for all positions the finger can operate inside these quadrants.

Once obtained, the x value is replaced in Eq. (13), and with this point, P_{a1} is obtained.

Angle θ_2 (see Fig. 3) is defined by Eq. (15).

$$\theta_2 = \beta - \theta_1 - \alpha \tag{15}$$

In Fig. 4, it is observable that when $\theta_1 = 0$, the result is $\beta = \alpha$. and in Eq. (16), it is represented as β as the direction of the vector $\overrightarrow{P_{a1} - P_{f1}}$. Therefore:

$$\alpha = \tan^{-1}\left(\frac{(\overrightarrow{P_{a1} - P_{f1}})\hat{\jmath}}{(\overrightarrow{P_{a1} - P_{f1}})\hat{\imath}}\right) \tag{16}$$

With the mathematical model that defines the trajectory of the mechanism and the kinematic analysis that relates the dimensions of the links with the movement and the angles, an optimization problem can be formulated. In this case, it is a question of finding suitable dimensions for the links that allow complying with a trajectory profile without producing singularities or collisions. For this, the mathematical model and kinematic analysis will be necessary. The following section explains the optimization process.

3) Design parameters for the GA implementation

GA is an optimization biological inspired algorithm. This one is based on natural behavior, which constantly searches for an optimal state with the minimum effort. These algorithms are employed in the global optimization field (and in some other functions). They aim to find the best results as possible $x^*$of a space X with all events $F = f_1, f_2, \dots, f_n$. These events are generally represented like a mathematical expression in the function of the chosen variables [43].

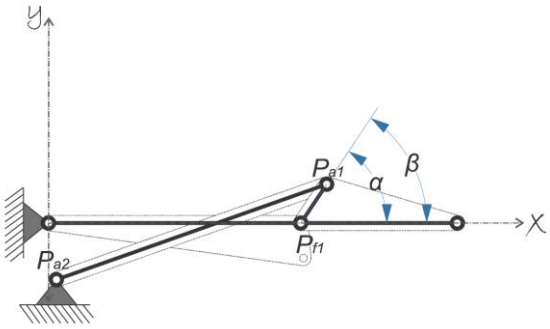

Figure 4. Estimation of angle α.

In this approach, the algorithm's chosen variables are unknown values (dimensions) of mechanisms previously analyzed. The parameters used in this method are shown in Table II.

TABLE II. PARAMETERS FOR THE GA IMPLEMENTATION.

Input Data	Value
The population size	30
The maximal generation	1500
The variable number (Nvars): ($P_{a2}\hat{\imath}$, $P_{a2}\hat{\jmath}$, L_{a1}, and L_{b1}) two mechanisms.	8
Fitness scaling	Rank
Selection function	Stochastic uniform
Reproduction (elite count)	2
Reproduction (crossover fraction)	0.15
Mutation function	Adaptive feasible
Crossover heuristic ratio	1.2
Migration forward (fraction)	0.2
Migration forward (interval)	20
Stop criteria (generations)	1500
Stop criteria (stall generations)	500

If coming back to the previous subsection, it is possible to observe that these values are, $P_{a2}\hat{\imath}$, $P_{a2}\hat{\jmath}$, L_{a1}, and L_{b1}. Given that the mechanical system of a finger is composed of two of the analyzed mechanisms in a connected way, the total number of choice variables is eight. The event that must accomplish this optimization is the reduction of Metter Square Error (MSE) obtained by comparing the trajectory in the developed task space by the mechanism with the proposed trajectory and the angles relations of Cobos (See Eqs. (1) and (2)).

Fig. 5 illustrates three curves in their graphic order, the first is the objective curve of movement in the task space, calculated from the relation of Cobos angles [23]. In his study, the second one is the curve generated with randomly selected values for the links (the exact curve in Fig. 2). It is possible to see that the error of the second curve is very high concerning the objective curve. Finally, there is a curve of 32 tries improved with GA. In this approach, the algorithm GA was employed with 300 iterations for each attempt and a population of 30 particles. It is essential to consider that GA is a heuristic algorithm, this fact does not assure the possibility of finding the exact solution for each attempt.

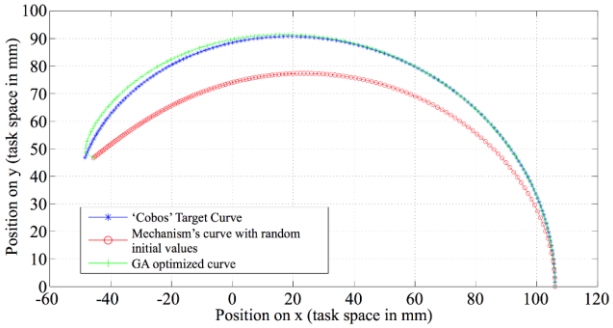

Figure 5. Trajectory curves simulated.

In Fig. 6, it is possible to observe the evolution of MSE inside the 300 iterations of each one of the 32 improvement tries. The minimal error achieved in the 32 tries was one of 0.0037. The best improvement is the one that can be visualized in Fig. 5.

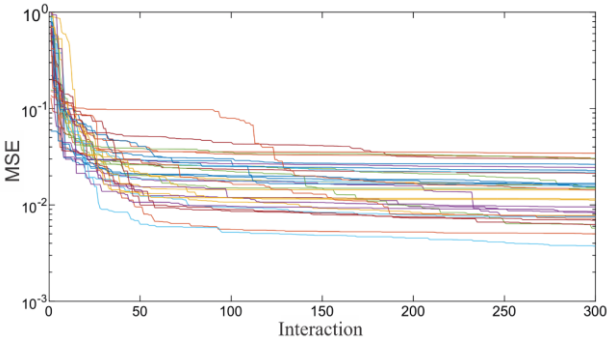

Figure 6 Convergency of MSE in the 32 optimization attempts during the 300 iterations.

The objective function makes it possible to find the minimum values of the parameters ($P_{a2}\hat{\imath}$, $P_{a2}\hat{\jmath}$, L_{a1}, and L_{b1}) that determine the correct dimensions of the finger mechanism to comply with a specific tray sector profile for the grip of the hand. Defining the minimum dimensional parameters of ManUPA allows you to carry out an adjusted mechanical design, select precise components and reduce manufacturing costs. The objective function outputs a numerical performance value from the MSE calculation obtained when comparing the trajectory in the workspace developed by the mechanism with the proposed trajectory and relating the angles that define the movement. Fig. 6 shows the behavior of the objective function in 32 improvement attempts, it is observed that it seeks to find the minimum adequate dimensions to comply with the profile of the tray sector that defines the type of grip, the algorithm converges by what changes in the values in the produce significant difference in the yield measure.

4) Finger's results

The fingertip trajectory was simulated and compared with the objective curve of each finger, as seen in Fig. 5. In Fig. 7, A mechanism simulation is observed, and each inter-phalanx joint performs the movement in the task space. It is observable that the movement is very close to being lineal, which was the optimization's aim goal, considering that the relations of movements proposed by Cobos are also observable [42].

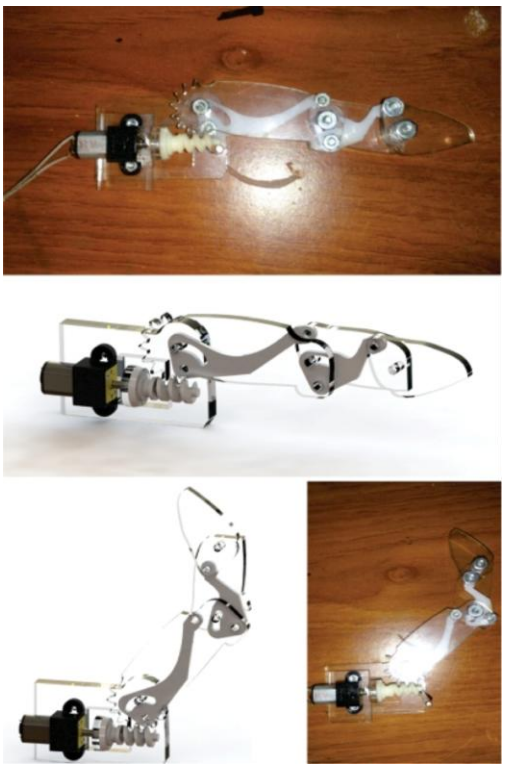

Figure 7. Simulation of a designed finger.

In the beginning, a prototype was designed to analyze its movement in real life, undertake the corresponding proof of the interference among links, and find the possible errors of design that were out of the simulation stage. The result of this first finger prototype is illustrated in Fig. 8.

In the final version, plenty of aspects were considered and discovered thanks to the construction of this prototype. Such as the necessity of support for the other extreme of the endless screw or even mechanism tolerance.

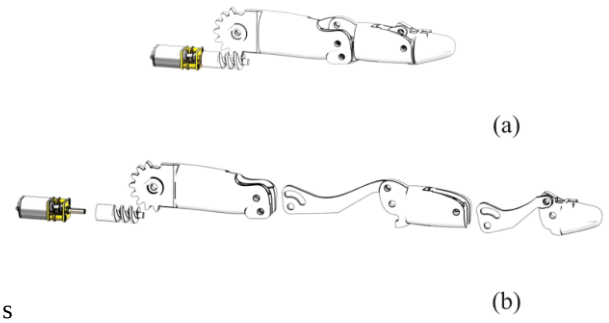

s

Figure 8. Printed finger in 3D. (a) Assembled finger view. (b) Exploited finger view.

B. Robotic Multi-finger Hand Design

In this section, the mechanism improved and simulated in the previous stage is more deeply designed. It is crucial that the Computer-aided Design (CAD) picture stays true to the model and that the mechanism is similar to a human finger. Once the conceptual design of a finger is proven, it is time to proceed to develop the design kept in mind in its construction in a 3D printer where more complex pieces could be constructed and even more similar to a human finger.

1) Pinky, ring, and middle fingers

Considering its kinematic nature, the design of Little, Ring, and Middle fingers have been grouped in the same slot, all fingers were created using the same principle (see Fig. 9). The only change was the measures of their links that were improved in the previous chapter. The finger was designed to show as less as possible the mechanism and be as rigid as possible, trying to reduce the weaknesses of mechanical games.

2) Index

Index design, as thumb design, was undertaken independently because of these active adductions and abduction movements. Mechanism's kinematics allow flexion and extension movements the same as the one of Ring, Middle, and Little, nevertheless, it was necessary to add another mechanism that allows adduction and abduction movements around the axis shown in Fig. 9(a), transmitting movements through conical gears.

In Fig. 9(b), it is possible to appreciate the base designed especially for the index. Regarding its kinematic features, it was necessary to make a groove to enter the micro engine, the endless screw, and another groove for a potency gauge used to support the finger's position.

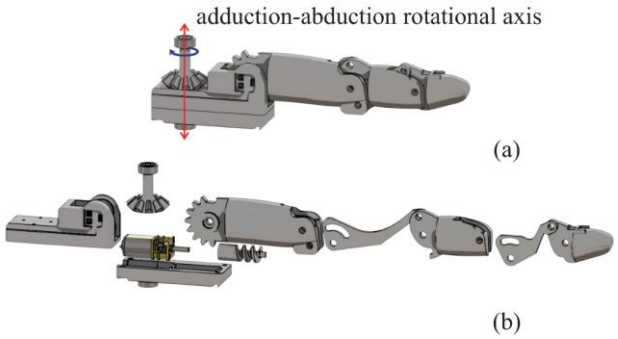

Figure 9. Index. (a) Assembled finger view; (b) Exploited finger view.

3) Thumb

Thumb neutral or resting muscular positions, defined by C. Hammonet and P. Valentin, are the vector position that can be appreciated in Fig. 10. This position corresponds to the silence electromyography position: where no thumb muscle reflects the potential of action [44].

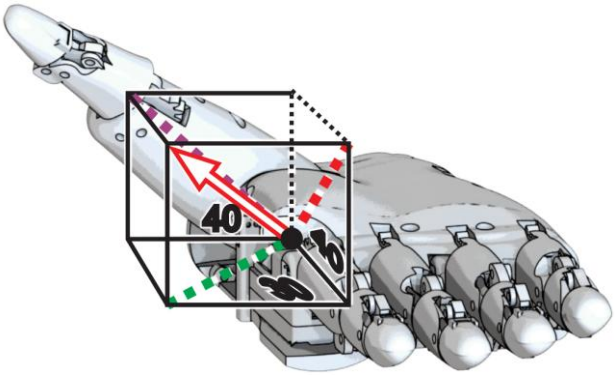

Figure 10. Thumb design and orientation.

Fig. 10 also illustrates the design results for the thumb's base, which can rotate around the axis illustrated in Fig. 11. The importance of the thumb's opposition movements is one feature that gives a human hand more dexterity. Its use and importance are reflected in the section on results, where a discussion will be presented later on.

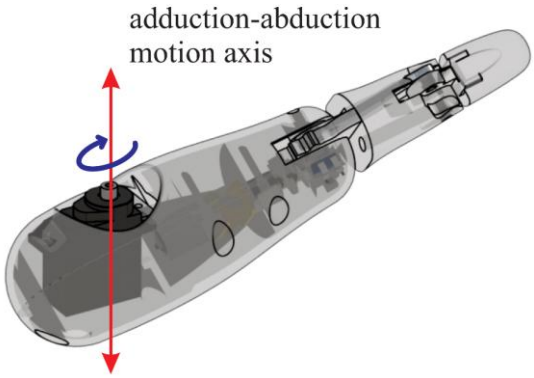

Figure 11. Thumb and base.

4) *Hand's construction and design results*

Fig. 12 compares the results of the robotic hand CAD performing a gesture in which the thumb's opposition is tested.

Table III present the physical dimensions that form a robotic hand. The hand size is about *208×223* mm and weighs *400* gr approximately.

TABLE III. PHYSICAL DIMENSIONS OF MANUPA

Dimension	Size [mm]	
	Thumb Adducted	Thumb Abducted
Length	208	102
Width	54	153
Height	223	-

The ManUPA prototype of a robotic hand has 16 joints, of which seven are performed, and the others are sub-performed. Fig. 12 illustrates the location of all of those included in the prototype. Those in red are joints performed using electric engines, and those in black are sub-performed joints using four sticks presented in the previous section.

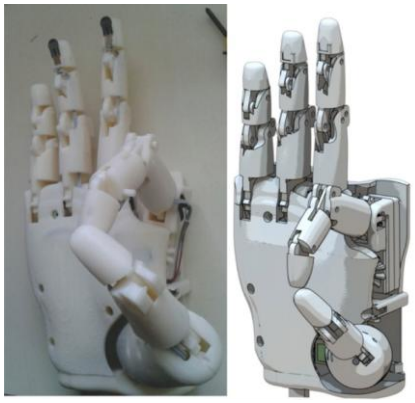

Figure 12. Assembled hand results.

Table IV presents the motility relations of the joints presented in Fig. 13, joined to their angular limitation movements. Table IV is divided into columns for the kinematic connection present in the different fingers previously presented. Then, they are sub-divided into a section that marks the prototype's angular relation with the same nomenclature found in Fig. 13 and each articulation's angular limitations. Evenly the order of these inter-phalanx joints of the hand are: trapezium metacarpal of adduction and abduction ($\theta_{X,TMC_{aa}}$), proximal metacarpal of adduction and abduction ($\theta_{X,MCP_{aa}}$), proximal inter phalanx ($\theta_{X,PIP}$) and distal inter phalanx ($\theta_{X,DIP}$).

TABLE IV. INTERPHALANGEAL RELATIONS OF THE MANUPA PROTOTYPE MOVEMENTS.

Thumb		Index		Fingers with 1-DOF			
				Middle	Ring	Pinky	Limits
Relation	Limits	Relation	Limits	Relation			
$\theta_{P,TMC_{aa}}$	0-90 °	-	-	-	-	-	-
-	-	$\theta_{I,MCP_{aa}}$	0-60 °	-	-	-	-
$\theta_{P,MCP_{fe}} \approx \frac{4}{3}\theta_{P,IP}$	0-90 °	$\theta_{I,MCP_{fe}} \approx \frac{4}{3}\theta_{I,PIP}$	0-90 °	$\theta_{C,MCP_{fe}} \approx \frac{4}{3}\theta_{C,PIP}$	$\theta_{A,MCP_{fe}} \approx \frac{4}{3}\theta_{A,PIP}$	$\theta_{M,MCP_{fe}} \approx \frac{4}{3}\theta_{M,PIP}$	0–90 °
$\theta_{P,IP}$	0-67.5	$\theta_{I,PIP} \approx \frac{3}{2}\theta_{I,DIP}$	0-67.5 °	$\theta_{C,PIP} \approx \frac{3}{2}\theta_{C,DIP}$	$\theta_{A,PIP} \approx \frac{3}{2}\theta_{A,DIP}$	$\theta_{M,PIP} \approx \frac{3}{2}\theta_{M,DIP}$	0–67.5 °
-	-	$\theta_{I,DIP}$	0-45 °	$\theta_{C,DIP}$	$\theta_{A,DIP}$	$\theta_{M,DIP}$	0–45 °

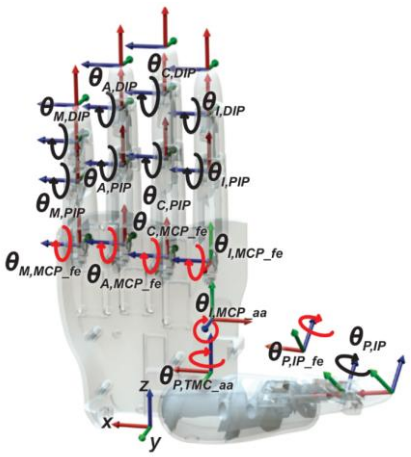

Figure 13. Description of joint movements of the complete robotic hand. In red color are shown the performed articulations and in black color the sub-performed articulations.

C. Hardware and Prototype Control

The only physical and mechanical constitution of the ManUPA prototype has been described. However, this prototype is also composed of diverse electric, electronic, and electro-mechanic components for its functionality. In addition to this, those components require control algorithms and a specific protocol to allow ManUPA to perform the different movements and gestures. These prototype components, their internal system of connections, and the protocol followed to control them are presented in this section.

1) Hardware

Electric engines of reduced sizes are in charge of rotation movements of articulations performed by the ManUPA prototype. For the flexion and extension movements of the five fingers, Micro engines HP100: 1 were selected because they support a nominal voltage of 6V and the following features: 320 RPM, 80 mA with a free axis, 2.2 kg–cm of exit torque, and 1 A with the stopped axis. For movements of adduction and abduction of fingers, thumb, and index servo engines HD-1810MG (6V: 0.13 sec/60 ºof speed, 3.9 kg-cm of exit torque) have been selected. The most critical feature of these selected engines is their reduced size in relation to their pair.

This prototype has two kinds of sensors in its system:

- Location sensors for fingers: they are tiny rheostats, placed in the proximal metacarpal axis of flexion-extension ($\theta_{X,MCP_{fe}}$) of each finger (see Fig. 14). There are 5 of these sensors implemented in ManUPS (one for each finger).
- Resistive force sensors: to understand in a better was the robotic hand in terms of its external structure, some tactile force generators have been added to the fingertips. The strategic position in this area allows ManUPA to perform precision grip movements.

To control the mini card of development A-Star 32 Ua4, Mini LV was selected, this is a development card with a microcontroller named Atmel-32U3. When choosing this device, the number of pins used in this process, the processing speed, and size reduction were vital factors. In Fig. 14, it is possible to see that approximately 95% of its pins were employed in this card.

2) Study's control and flow chart

As mentioned before, the board A-Star 32U4 Mini LV is included in the ManUPA prototype. Among its functions, it is possible to find:

- Receive control instructions: there are three types of instructions; (1) change the "set point" of one performed joint (see Fig. 14) with any angular position (in grades), (2) read force sensors, and (3) read placement sensors.
- PI articulation controller of flexion and extension: once the prototype is turned on, set points of all fingers are reactivated, and these could then be modified with control instructions. Control signal towards the engine via PWMs (Pulse Width Modulation).
- Control signal transducer for articulations of adduction and abduction: as mentioned before, adduction and abduction articulations of the ManUPA prototype are activated by micro servos. When they are given the order to change the set point of any of these joints, the card generates a Pulse width modulation (PWM) signal corresponding to the one that is sent to the driver of each servo engine.
- Force sensors signal transducer: the card transforms analogical force sensor's signal in pressing unities (Kgf/cm^2).

Fig. 14 illustrates the graphic connections of the control card. Electric, electronic, and electro-mechanic components can also be visualized, these components are the ones that form the prototype and the signal they employ to work.

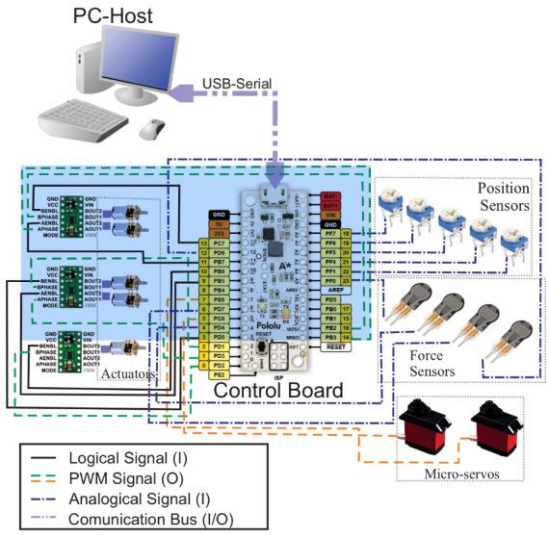

Figure 14. Connection map and data and signals flow in the ManUPA prototype.

Control instructions are sent to the hand through a host serial–USB and a BaudRate of 115200. This host could be a personal computer or a robotic control system. It is essential to highlight that it is only necessary to have a USB connection. By simple instructions with any communication serial, the hand can be controlled and adapted to any application (it does not need external control or reference commands).

IV. Results and Discussion

Figs. 15–16 make it possible to visualize the hand performing different kinds of grip, which are typical to the human hand. These movements are performed in the handgrip taxonomy proposed by Cutkosky [47, 48].

Figure 15. Power prismatic grip with greater diameter

Fig. 16 shows an excellent potency grip used to grab big objects, this kind of grip lacks skillfulness. Meanwhile, Fig. 16(a) introduces a kind of grip that is performed. It is necessary to grip small objects with tremendous pressure. It represents a skilled grip testing the utility of the thumb's inhibition thanks to adduction and abduction movements included in the hand, in Fig. 16(b). It is possible to observe the importance of this movement when emulating different gestures and grips with the hand.

Regarding adduction importance and abduction movements, the human hand in Fig. 16(a) and Fig. 16(d) also shows the relevance of these movements in the index, the grips illustrated would not have been possible without this degree of freedom.

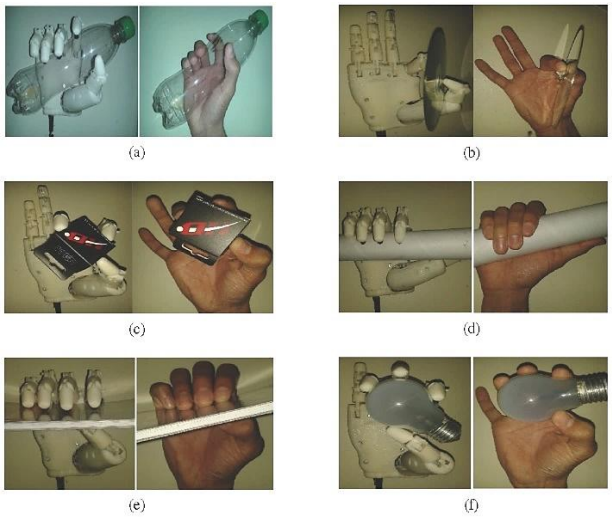

Figure 16. The hand performing different kinds of grip (a) Power prismatic grip with the thumb abducted (b) Power prismatic grip with the thumb abducted (c) Precision prismatic grip with 2 fingers (Thumb and index) (d) Precision prismatic grip with 3 fingers (thumb, index and middle finger) (e) Precision prismatic grip with 4 fingers (thumb, index, middle and ring fingers) (f) Circular grip of tripod accuracy.

TABLE V. THE ERROR INDEX FOR TRACKING A TRAJECTORY PROFILE

Grip type	Types of DOF compared	
	7–DOF	9–DOF
Prismatic	9.10%	5.90%
Circular	13.2%	7.65%

It is possible to compare the developed ManUpa that has 7–DOF concerning the performance of the grip type to other models of simplified 9–DOF robotic hands. The prismatic types of grip are contemplated in this research. Fig. 16 shows the different types of grip considered in this comparison. An ideal trajectory profile that can be achieved with 24–DOF hands is used to calculate the trajectory tracking error. Table V presents the result of the comparison made. Estimating that the applications projected for ManUpa tolerate a permissible error of 10% and the calibration processes are adequate to take advantage of the maximum capacity, it can be deduced that the type of operation is sufficient for these activities. If precision requires less than 5% tolerances, a hand with more degrees of freedom will be adequate for these tasks. It is determined that the ManUPA performs better in circular-type grips.

V. CONCLUSION

This research presented the development of a multi-fingered robotic hand with a size that is only 10% greater than the dimensions and extension of a natural human hand. The hand features a simplified 7–DOF rigid bar mechanism, 16 joints, and a maximum force of 24N. The mechanism follows a defined tray sector profile to control different grip types. The control system and its actuators are located in the palm, representing a straight integration of the system in a reduced space. The intended objective was met, which consisted of simplifying the construction of the robotic hand to be used as an end effector in tasks that require dexterity. Even with variants in the grip control system, the application possibilities could be numerous. The control strategy links feedback through tactile and force sensors placed on the fingers of the ManUPA prototype, with position control, but more complex controllers can be applied. The addition of these sensors makes it possible to understand the implementation of different advanced manipulation techniques, such as impedance and power control.

It was established as a method of validation and comparison of the tracking of the tray sector defined for the type of grip, which, based on an optimization result and combined with the joint control system, provides a kinematic performance of the proposed mechanism to be used as fine grip systems. Different grips presented in this document demonstrate the dexterity of the hand, given by the type of rigid mechanism and the tracking of the tray sector profile. The movements of adduction and abduction of the hand expand their usefulness to reproduce different types of grips. It is necessary to emphasize that this achievement was possible thanks to the design configuring the thumb's base. In related literature and similar studies, the thumb is generally placed on the opposite side of the palm. This feature is inappropriate to install because it will not allow an optimal grip when needed.

CONFLICT OF INTEREST

The authors declare no conflict of interest.

AUTHOR CONTRIBUTIONS

Sergio Pertuz and Cesar Peña conducted the research; Cristhian Riaño analyzed the data and wrote the paper; all authors had approved the final version.

REFERENCES

[1] C. Piazza, G. Grioli, M. G. Catalano and A. J. A. R. O. C. Bicchi, "A century of robotic hands," *Annual Review of Control, Robotics, and Autonomous Systems,* vol. 2, pp. 1–32, 2019.

[2] L. Biagiotti, F. Lotti, C. Melchiorri, and G. Vassura, "How far is the human hand? a review on anthropomorphic robotic end-effectors," *University of Bologna, Tech. Rep,* 2004.

[3] M. Hernando, C. Morillo, D. Guffanti and A. Brunete, "Mechatronic design of a self-contained dexterous robotic hand for

gestural communication," *International Journal of Social Robotics*, pp. 1–11, 2023.

[4] M. S. Johannes, J. D. Bigelow, J. M. Burck, S. D. Harshbarger, M. V. Kozlowski, and T. Van Doren, "An overview of the developmental process for the modular prosthetic limb," *Johns Hopkins APL Technical Digest*, vol. 30, pp. 207–216, 2011.

[5] M. Laffranchi, N. Boccardo, S. Traverso, L. Lombardi, M. Canepa, A. Lince, M. Semprini, J. A. Saglia, A. Naceri, R. Sacchetti, and others, "The Hannes hand prosthesis replicates the key biological properties of the human hand," *Science Robotics*, vol. 5, p. eabb0467, 2020.

[6] H. Liu, "Exploring human hand capabilities into embedded multifingered object manipulation," *IEEE Transactions on Industrial Informatics*, vol. 7, pp. 389–398, 2011.

[7] A. Bicchi, "Hands for dexterous manipulation and robust grasping: A difficult road toward simplicity," *IEEE Transactions on Robotics and Automation*, vol. 16, pp. 652–662, 2000.

[8] F. Cini, V. Ortenzi, P. Corke, and M. J. S. R. Controzzi, "On the choice of grasp type and location when handing over an object," *Science Robotics*, vol. 4, p. eaau9757, 2019.

[9] M. A. Roa and R. Suárez, "Grasp quality measures: Review and performance," *Autonomous Robots*, vol. 38, pp. 65–88, 2015.

[10] S. R. Kashef, S. Amini, and A. Akbarzadeh, "Robotic hand: A review on linkage-driven finger mechanisms of prosthetic hands and evaluation of the performance criteria," *Mechanism and Machine Theory*, vol. 145, p. 103677, 2020.

[11] C. Piazza, M. G. Catalano, S. B. Godfrey, M. Rossi, G. Grioli, M. Bianchi, K. Zhao, and A. Bicchi, "The softhand pro-h: a hybrid body-controlled, electrically powered hand prosthesis for daily living and working," *IEEE Robotics & Automation Magazine*, vol. 24, pp. 87–101, 2017.

[12] J. L. Pons, R. Ceres, and F. Pfeiffer, "Multifingered dextrous robotics hand design and control: A review," *Robotica*, vol. 17, pp. 661–674, 1999.

[13] M. A. Devi, G. Udupa, and P. Sreedharan, "A novel underactuated multi-fingered soft robotic hand for prosthetic application," *Robotics and Autonomous Systems*, vol. 100, pp. 267–277, 2018.

[14] X. Zhou, C. Majidi, and O. M. O'Reilly, "Soft hands: An analysis of some gripping mechanisms in soft robot design," *International Journal of Solids and Structures*, vol. 64, pp. 155–165, 2015.

[15] R. Ozawa and K. Tahara, "Grasp and dexterous manipulation of multi-fingered robotic hands: A review from a control view point," *Advanced Robotics*, vol. 31, pp. 1030–1050, 2017.

[16] N. Govindan, S. S. V. Kovvali, K. Chandrasekaran, and A. Thondiyath, "GraspMan-a novel robotic platform with grasping, manipulation, and multimodal locomotion capability," in *Proc. 2018 IEEE International Conference on Robotics and Automation (ICRA)*, 2018.

[17] A. Schmitz, U. Pattacini, F. Nori, L. Natale, G. Metta, and G. Sandini, "Design, realization and sensorization of the dexterous iCub hand," in *Proc. 2010 10th IEEE-RAS International Conference on Humanoid Robots*, 2010.

[18] S. H. Jeong, K. S. Kim, and S. Kim, "Designing anthropomorphic robot hand with active dual-mode twisted string actuation mechanism and tiny tension sensors," *IEEE Robotics and Automation Letters*, vol. 2, pp. 1571–1578, 2017.

[19] M. Grebenstein, A. Albu-Schäffer, T. Bahls, M. Chalon, O. Eiberger, W. Friedl, R. Gruber, S. Haddadin, U. Hagn, R. Haslinger, et al., "The DLR hand arm system," in *Proc. 2011 IEEE International Conference on Robotics and Automation*, 2011.

[20] C. H. Xiong, W. R. Chen, B. Y. Sun, M. J. Liu, S. G. Yue, and W. B. Chen, "Design and implementation of an anthropomorphic hand for replicating human grasping functions," *IEEE Transactions on Robotics*, vol. 32, pp. 652–671, 2016.

[21] N. J. Jarque-Bou, M. Vergara, J. L. Sancho-Bru, V. Gracia-Ibáñez, and A. Roda-Sales, "Hand kinematics characterization while performing activities of daily living through kinematics reduction," *IEEE Transactions on Neural Systems and Rehabilitation Engineering*, vol. 28, pp. 1556–1565, 2020.

[22] L. E. Sánchez-Velasco, M. Arias-Montiel, E. Guzmán-Ramírez, and E. Lugo-González, "A low-cost emg-controlled anthropomorphic robotic hand for power and precision grasp," *Biocybernetics and Biomedical Engineering*, vol. 40, pp. 221–237, 2020.

[23] S. Cobos, M. Ferre, M. S. Uran, J. Ortego, and C. Pena, "Efficient human hand kinematics for manipulation tasks," in *Proc. 2008 IEEE/RSJ International Conference on Intelligent Robots and Systems*, 2008.

[24] S. A. Pertuz, C. H. Llanos, and D. M. Muñoz, "Development of a robotic hand using bioinspired optimization for mechanical and control design: UnB-Hand," *IEEE Access*, vol. 9, pp. 61010–61023, 2021.

[25] D. R. Biswal and P. K. Parida, "Design and kinematic analysis of an anthropomorphic underactuated robotic hand for orthopaedic rehabilitation," *Journal of Pharmaceutical Negative Results*, pp. 2444–2456, 2022.

[26] X. Li, Z. Chen, and C. Ma, "Optimal grasp force for robotic grasping and in-hand manipulation with impedance control," *Assembly Automation*, vol. 41, pp. 208–220, 2021.

[27] C. T. Lee and J. Y. Chang, "A workspace-analysis-based genetic algorithm for solving inverse kinematics of a multi-fingered anthropomorphic hand," *Applied Sciences*, vol. 11, p. 2668, 2021.

[28] A. Pérez-González and I. Llop-Harillo, "Optimization of the kinematic chain of the thumb for a hand prosthesis based on the kapandji opposition test," in *Proc. 16th International Symposium CMBBE and 4th Conference on Imaging and Visualization on Computer Methods, Imaging and Visualization in Biomechanics and Biomedical Engineering*, August 14-16, 2019, New York City, USA, 2020.

[29] S. A. Pertuz, C. H. Llanos, and D. M. Munoz, "Bioinspired optimization of a robotic finger mechanism," in *Proc. 2016 XIII Latin American Robotics Symposium and IV Brazilian Robotics Symposium (LARS/SBR)*, 2016.

[30] G. A. Bekey, R. Tomovic, and I. Zeljkovic, "Control architecture for the Belgrade/USC hand," *Dextrous Robot Hands*, pp. 136–149, 1990.

[31] N. Fukaya, S. Toyama, T. Asfour, and R. Dillmann, "Design of the TUAT/Karlsruhe humanoid hand," in *Proc. 2000 IEEE/RSJ International Conference on Intelligent Robots and Systems (IROS 2000)(Cat. No. 00CH37113)*, 2000.

[32] C. S. Lovchik And M. A. Diftler, "The Robonaut Hand: A Dexterous Robot Hand For Space," In *Proc. 1999 Ieee International Conference on Robotics And Automation (Cat. No. 99ch36288c)*, 1999.

[33] S. Schulz, C. Pylatiuk, and G. Bretthauer, "A new ultralight anthropomorphic hand," in *Proc. 2001 ICRA. IEEE International Conference on Robotics and Automation (Cat. No. 01CH37164)*, 2001.

[34] H. Kawasaki, T. Komatsu, and K. Uchiyama, "Dexterous anthropomorphic robot hand with distributed tactile sensor: Gifu hand II," *IEEE/ASME Transactions on Mechatronics*, vol. 7, p. 296–303, 2002.

[35] H. Liu, K. Wu, P. Meusel, N. Seitz, G. Hirzinger, M. H. Jin, Y. W. Liu, S. W. Fan, T. Lan, and Z. P. Chen, "Multisensory five-finger dexterous hand: The DLR/HIT Hand II," in *Proc. 2008 IEEE/RSJ International Conference on Intelligent Robots and Systems*, 2008.

[36] D. H. Lee, J. H. Park, S. W. Park, M. H. Baeg, and J. H. Bae, "KITECH-hand: A highly dexterous and modularized robotic hand," *IEEE/ASME Transactions on Mechatronics*, vol. 22, pp. 876–887, 2016.

[37] U. Kim, D. Jung, H. Jeong, J. Park, H. M. Jung, J. Cheong, H. R. Choi, H. Do, and C. Park, "Integrated linkage-driven dexterous anthropomorphic robotic hand," *Nature Communications*, vol. 12, p. 7177, 2021.

[38] H. Zhou, C. Tawk, and G. Alici, "A 3D printed soft robotic hand with embedded soft sensors for direct transition between hand gestures and improved grasping quality and diversity," *IEEE Transactions on Neural Systems and Rehabilitation Engineering*, vol. 30, pp. 550–558, 2022.

[39] R. Deimel and O. Brock, "A novel type of compliant and underactuated robotic hand for dexterous grasping," *The International Journal of Robotics Research*, vol. 35, pp. 161–185, 2016.

[40] R. Ma and A. Dollar, "Yale openhand project: Optimizing open-source hand designs for ease of fabrication and adoption," *IEEE Robotics & Automation Magazine*, vol. 24, pp. 32–40, 2017.

[41] O. Binvignat, A. Almagià, P. Lizana, and E. Olave, "Biometric aspects of the hand of Chilean individuals," *International Journal of Morphology*, vol. 30, pp. 599–606, 2012.

[42] S. C. Guzmán, *Analysis of Virtual Manipulation Tasks Based on Reduced Models of the Human Hand*, Madrid España: Universidad Politecnica de Madrid, 2010.

[43] T. Weise, "Global optimization algorithms-theory and application," *Self-Published Thomas Weise*, vol. 361, 2009.

[44] A. Kapandji and M. Torres, "Articular physiology: Commented schemes of articular mechanics. shoulder, elbow, pronosupination, wrist, hand. 1," *Articular Physiology*, vol. 1.

[45] M. R. Cutkosky, et al., "On grasp choice, grasp models, and the design of hands for manufacturing tasks," *IEEE Transactions on Robotics and Automation*, vol. 5, pp. 269–279, 1989.

[46] M. Cutkosky and P. Wright, "Modeling manufacturing grips and correlations with the design of robotic hands," in *Proc. 1986 IEEE International Conference on Robotics and Automation*, 1986.